Seismic response of half-scale seven-storey RC systems with torsional irregularities: blind prediction

T. Suzuki & K.J. Elwood
The University of Auckland, Auckland.

A.Y. Puranam
National Taiwan University, Taipei, Taiwan.

H-J. Lee
National Yunlin University of Science and Technology, Yunlin, Taiwan.

F-P. Hsiao & S-J. Hwang
National Center for Research on Earthquake Engineering, Taipei, Taiwan.

ABSTRACT

Past earthquakes have highlighted vulnerabilities to damage or collapse of building structures due to torsional response. While methodologies to capture torsional demand due to strength and stiffness irregularities have been studied in detail in the past, there is uncertainty in determining the effect of torsion associated with nonlinear seismic response. This study aims to investigate inelastic torsional response of existing concrete buildings through experiments. Two half-scale seven-storey structures were tested on an earthquake simulator at NCREE Tainan Laboratory. The tested structures were subjected to uni-directional excitation. The first specimen, with ductile detailing, was designed to study: i) Stiffness irregularity and ii) Damage irregularity. The second specimen simulated as a system with iii) Non-ductile irregularity. A blind prediction competition was held to predict the response of these test structures to a series of ground motion excitations. This paper summarises the test programs and presents a comparison of the test results and predictions from the competition.

1 INTRODUCTION

After past earthquakes, a number of reinforced concrete (RC) building structures have been rendered unusable because of collapse or localized damage to structural elements. In some cases, post-earthquake investigations reported that the localization of damage was caused by irregularities in the structural systems and torsional response. In most cases, the irregularities resulted from unsymmetrical alignment of primary or secondary structural elements in plan. The resulting torsional eccentricity from stiffness irregularity is the most common parameter used in both new design standards and assessment guidelines. In addition to stiffness irregularity, design standards and guidelines define accidental eccentricity as 0% to 10% of the plan dimension perpendicular to the considered lateral force resisting system. This method provides a conservative buffer for torsional effects not directly accounted for in the modelling of the building. Past studies (e.g. Llela and Chopra, 1995) proposed methodologies to assess the accidental eccentricity based on contributing ratio of torsional modes to translational modes. Despite the improvement in considering torsional demand in design and assessment, we have yet to obtain sufficient experimental data to confirm that the theory sufficiently represents the torsional response of new/existing RC buildings, specifically when nonlinear behaviour is expected.

Paulay (2001) and related studies (e.g. Paulay, 1998; Castillo, 2004) established static design theory for inelastic torsion in ductile systems, which accounted for strength eccentricities in addition to stiffness eccentricities. The concept of strength irregularity is reflected in New Zealand Seismic Assessment Guidelines, (NZSEE, 2017). Yet there is paucity of experimental data related to the effect of inelastic torsion on displacement demands in these systems. In fact, the strength eccentricity still relies on the original state of structures and hence may not be sufficient to assess nonlinear torsion when strength deterioration of structural elements is expected. Existing RC buildings are also considered particularly sensitive to torsion because of structural weaknesses, such as the use of brittle elements or concentrated demands at soft or weak storeys. The aim of this study is to evaluate whether numerical simulations recommended in the assessment guidelines capture the displacement demands in buildings experiencing inelastic torsional response, and also to improve methods in existing guidelines.

This study aims to investigate inelastic torsional response of concrete buildings through physical experiments and numerical analyses. The test program includes shake-table testing of two half-scale, 7-storey RC specimens (Specimen-1 and Specimen-2) at the Tainan laboratory of National Center for Research on Earthquake Engineering (NCREE), Taiwan. The two specimens have different sources of torsional irregularities and were designed considering the structural systems of RC residential buildings that collapsed during the 2016 Meinong Earthquake in Tainan, along with some modifications to adjust to the research needs. A blind prediction competition was held and this paper discusses the comparison of experimental results and blind analyses for the primary responses of the tested specimens.

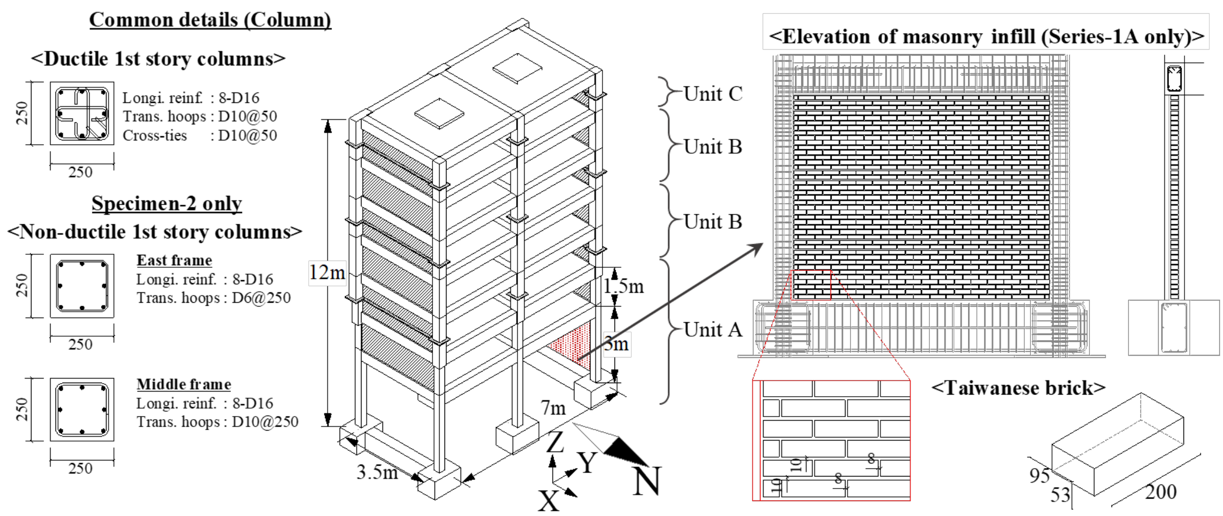

Figure 1: Overview of the test specimen

2 TEST PROGRAMS

2.1 Design of specimens

The two test structures, Specimen-1 and Specimen-2, were designed to study inelastic torsional response caused by different source of irregularities (illustrations shown in Table 1). The specimens were half-scale seven-storey structures as shown in Figure 1, made of three separate units (A, B, and C). In this project, only

Table 1: Summary of properties of shake-table specimens

Specimen		Specimen-1		Specimen-2
Test series name		Series-1A	Series-1B	Series-2
Source of torsional response		Stiffness irregularities	Damage irregularity	Non-ductile irregularity
Illustration of irregular systems		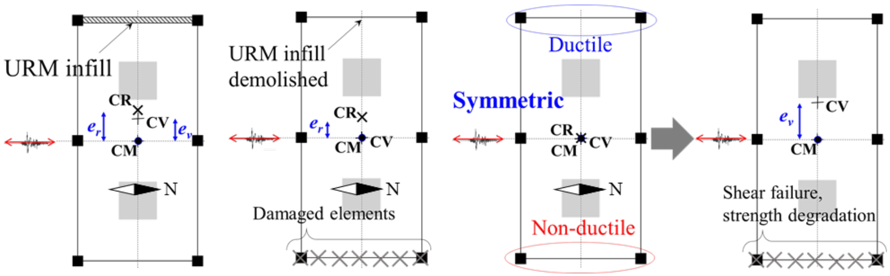		
Irregularity produced by		URM infill in West frame	Damage on East frame	Early strength degradation in East (non-ductile) frame
Columns (1^{st}-storey)	Dimensions	250 mm x 250 mm		
	Longi. Reinf.	2.6% from 8 D16 bars		
	Trans. Reinf. Ductile detailing	D10@50 mm hoops (135-degree hooks) and cross ties (180-degree hooks)		
	Trans. Reinf. Non-ductile detailing	N/A		D6 (East) or D10 (Middle)@250 mm hoops with 90-degree hooks
Beams (X-dir, 1^{st}-storey)	Dimensions	250 mm x 400 mm		
	Longi.Reinf.	Ends: 4 D16 top and bottom; Middle: 4 D16 top and bottom		
Beams (Y-dir, 1^{st}-storey)	Dimensions	250 mm x 450 mm		
	Longi. Reinf.	Ends: 6 D16 top and bottom; Middle: 4 D16 top and 6 D16 bottom		
Shear Walls	Thickness	150 mm		
	Reinforcement	Two layers of horizontal and vertical D10 bars @ 150mm		
Slabs	Thickness	100 mm		
	Reinforcement	Two-way D10 bars spaced @ 150 mm top and bottom		
Weight	Additional	2.3 ton (at each story from cast-in concrete block)		
	Total	136 ton (Including the base)		

Unit A – first two and a half storeys of each seven-storey structure – was newly constructed for each specimen. It was then connected with re-usable upper units (B and C) by boundary steel plates. Both specimens had a "soft" first storey with a height twice the height of the storeys above and RC shear walls in the short floor-plan direction (i.e. X-direction) in storeys 2 through 7. RC frames spanned one bay (3.5 m) along the short floor-plan direction and two bays (7 m) along the long floor-plan direction (Fig. 1). Table 1 summarises the details of both specimens, and Table 2 and Table 3 summarise the material properties of concrete and steel and masonry wall, respectively.

Table 2: Material properties of concrete and steel

Specification	**Concrete***	**D16 (SD420W)**		**D10 (SD280W)**		**D6 (JIS-SD345)**	
Specimen	**f'_c (MPa)**	**f_y (MPa)**	**f_u (MPa)**	**f_y (MPa)**	**f_u (MPa)**	**f_y (MPa)**	**f_u (MPa)**
Nominal	21	≥ 420	≥ 550	≥ 280	≥ 420	345-440	490
Speicmen-1	25.1*	468.7	667.8	334.3	445.3	N/A	N/A
Specimen-2	28.7*	459.7	650.9	351.3	458.2	379.3	500.6

*average of test-day strength, site curing

Table 3: Material properties of masonry components

Parameter	**Compressive strength of bricks (MPa)**	**Compressive strength of mortar (MPa)**	**Friction strength of mortar bed joint (MPa)**	**Compressive strength of masonry prism (MPa)**	**Shear strength of masonry panel (MPa)**
Tested strength	28.5	33.2 (bed joints) 52.4 (plaster)	0.76	12.2	0.66

As described in Table 1, columns at the first storey had a square cross-section measuring 250 mm x 250 mm and were reinforced with 8-D16 bars for a longitudinal reinforcement ratio of 2.6%. The first specimen was designed to explore the effect of: (i) torsional stiffness irregularity and (ii) damage irregularity. The columns in Specimen-1 included 'ductile' detailing as per NZS 3101:2006 to avoid brittle modes of failure and had transverse reinforcement made of D10 hoops and crossties spaced at 50 mm. To create the stiffness eccentricity, an unreinforced masonry (URM) infill wall was installed in the West frame at the first storey. The first series of tests (referred to as Series-1A) were conducted on this specimen with the expectation that the shaking would cause more damage on the East frame (the side without infill wall). Series-1A tests resulted in damage to the columns in the East frame while the West frame was effectively undamaged. The infill wall was demolished after Series-1A resulting in a structure with "damage irregularity" for the next series of tests (referred to as 'Series-1B').

The second specimen was designed to explore the effect of 'non-ductile' irregularity. Unit A of Specimen-2 was made identical to that of Specimen-1 except for the transverse reinforcement detail of four of the columns in the first storey. The columns on the East and the middle frames had D6 or D10 hoops at 250 mm, respectively (Fig. 1). Resulting ratio of plastic shear demand to shear strength (Sezen and Moehle, 2004) were 0.80 and 0.63 in East and Middle frames, indicating vulnerability to flexure-shear failures. The plastic shear demand to shear strength ratio for West frame was 0.18, indicating ductile response was expected. The asymmetric ductile detailing was selected to investigate the effect of "non-ductile irregularity", in which torsion was expected because of asynchronous strength degradation during strong shaking. The sequence of tests on Specimen-2 was referred to as ‘Series-2’.

2.2 Instrumentation

Twenty-three tri-axial accelerometers were connected to MTS FlexDAC^{TM} Data Acquisition System (referred to as FlexDAC) with a sampling rate of 512 Hz. Each floor had three accelerometers as shown in Figure 2 and the other two were placed on the base pedestals to record input motion. Positive-X, -Y and Z axes of these accelerometers corresponded to the axes shown in Figure 1. An optical measurement system by Optitrak^{TM}, referred to here as Motion Capture (MOCAP), was used to measure global displacements and local deformations. This system uses infrared cameras to capture three-dimensional coordinates of each reflective sphere or ‘target marker’. This study used 159 markers attached to the West, South and East surfaces of the specimen (shown as red, blue and green dots in Fig. 2). The data from MOCAP were recorded at a sampling rate of 128 Hz during each input. The red dots in the figure show markers placed at the centre line of beams and corners of diaphragm and these were used to capture storey drifts and rotation of the diaphragms. Markers on the base were used as reference to obtain relative displacements. In addition, some other markers placed on the table captured the movement of the simulator. The blue dots in the figure show the markers on first-storey columns installed to obtain the local deformations.

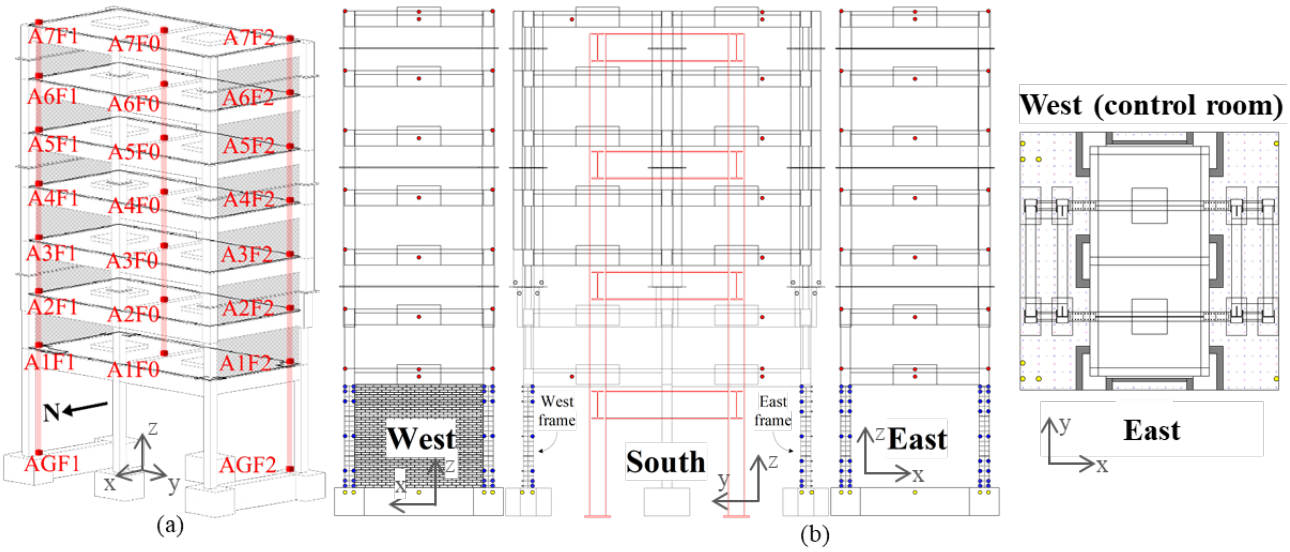

Figure 2: Drawings for instruments (a) Accelerometers and (b) MOCAP markers

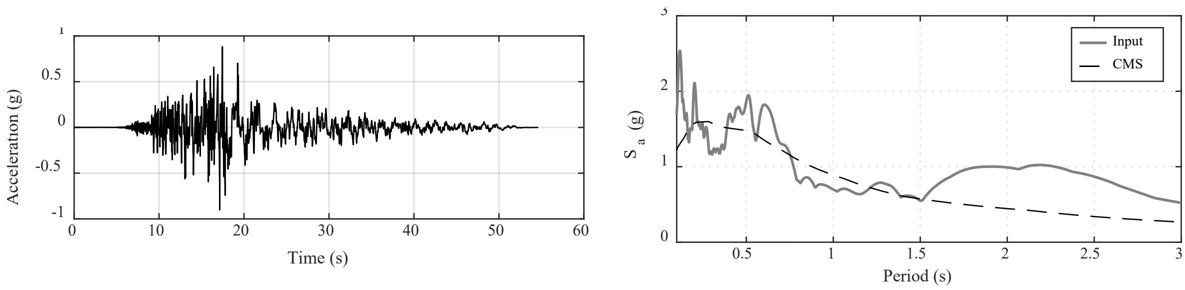

Figure 3: ‘100%’ input acceleration and acceleration spectrum

3 INPUT GROUND MOTION

The East-West component of the ground motion recorded at station CHY101 during 1999 Chi-Chi Earthquake, was selected for this testing program. This record is not only considered to represent typical near-fault records in Taiwan, but Tarbali & Bradley (2014) also included this same motion in a list of appropriate ground motions for a 'Wellington fault scenario' for Wellington, New Zealand. The original record, from the PEER Ground motion database, was time scaled by a factor of $1/\sqrt{2}$ (as the specimen is half-scale). The time-scaled record was also amplified in intensity by a factor of 2.65 to fit a 2500-year return period conditional mean spectrum in Wellington CBD using the scaling method proposed in Baker (2011). The resulting record scaled in time and intensity is referred to as the '100%' input or this testing program and has a peak ground acceleration and velocity of 0.90g and 1.22 m/s, respectively. The record was trimmed to exclude the first 9 seconds as the acceleration values were negligible (Fig. 3). Each series of tests (Series 1A, 1B and 2) consisted of a total of four earthquake inputs as shown in Table 4. A white noise test was done in between each input and at the beginning of the day.

Table 4: Earthquake input sequence

#	Series-1A (URM)		Series-1B (No URM)		Series-2 (Non-ductile)	
	Test name	**Scale**	**Test name**	**Scale**	**Test name**	**Scale**
1	1A-10%	10%	1B-10%	10%	S2-10%	10%
2	1A-20%	20%	1B-20%	20%	S2-20%	20%
3	1A-60%	60%	1B-40%	40%	S2-40%	40%
4	1A-60%-2	60%	1B-60%	60%	S2-60%	60%

Table 5: Deliverables for blind prediction

S/N	Deliverable	Symbol	Units
0	Fundamental period of the structure	T_s	sec
1a	Peak displacement of Frame-1 (relative to the table) in X-direction at first storey	$\delta_{X,1}$	mm
1b	Diaphragm rotation at first storey corresponding to 1a	$dRot_1$	rad
1c	Peak displacement (relative to the table) in Y-direction at first storey	$\delta_{Y,1}$	mm
1d	Peak displacement (relative to the table) in X-direction at the roof	$\delta_{X,\mathrm{R}}$	mm
1e	Diaphragm rotation at roof corresponding to 1d	$dRot_{\mathrm{R}}$	rad
1f	Peak displacement (relative to the table) in Y-direction at roof level	$\delta_{Y,\mathrm{R}}$	mm
2a	Maximum absolute acceleration in X-direction at geometric centre of first storey	$acc_{x,1}$	g
2b	Maximum absolute acceleration in X-direction at geometric centre of roof	$acc_{x,\mathrm{R}}$	g

4 BLIND PREDICTION COMPETITION

A blind prediction competition (QCBP 2019) was held by QuakeCoRE, New Zealand Centre for Earthquake Resilience, in collaboration with NCREE. The primary objective of the competition was to investigate the ability of different methods or software to estimate the demands on an RC structure subjected to torsion. Participants submitted entries under two categories: Category-1) non-linear response-history analysis, and Category-2) all other methods. This paper focuses on the results from Category-1 in which twelve teams participated. The website for the competition (http://www.quakecore.nz/blind-prediction-competition-2019/) provided general information about the experiments. Participants were given the acceleration in the X-direction obtained from AGF2 on the base pedestal for column at South-West corner (Fig. 2) recorded during the tests for Specimen-1. They were suggested to use the acceleration record from Series-1B for predicting the response in Series-2, as the weight of the specimens were identical. The recorded acceleration was processed by zero-phase digital filtering with fourth-order band-pass Butterworth IIR filter with the frequency range from 0.5 Hz to 30 Hz. In the competition, the participants were required to submit the deliverables as listed in Table 5. The authors also collected the histories of first-storey and roof displacement, acceleration at geometric centre and diaphragm rotation from the participants in Category-1. In addition, we requested each participant to submit the description of the analysis modelling technique and answer a short questionnaire.

According to the responses to the questionnaire (summarised in Fig. 4), six different academic and commercial software (e.g. OpenSees, SeismoStruct) were used. Eight teams out of the twelve modelled column elements with fibre sections (either force-based or displacement-based; i.e. FB or DB); therefore, most of the numerical models were able to account for interaction between the axial force and two-dimensional bending regardless of the type of analysis software. In addition, eight teams considered distributed mass while four used lumped masses (two out of the four put multiple lumped mass). There did not appear to be any significant differences in the main modelling assumptions; variation in prediction is therefore expected to come from computation and other detailed modelling.

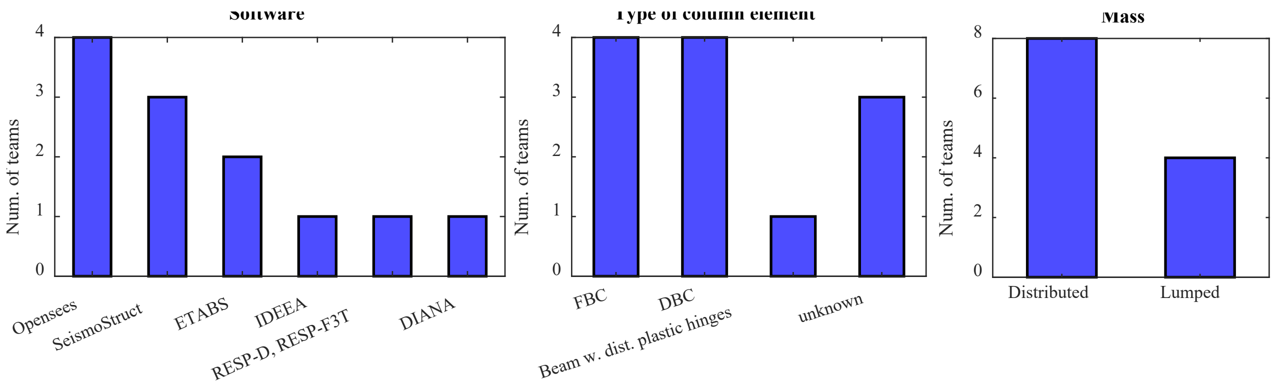

Figure 4: Summary of answers to the questionnaire

*Table 6: Measured test results**

Symbol (Unit)	1A-10%	1A-20%	1A-60%	1A-60%-2	1B-10%	1B-20%	1B-40%	1B-60%	S2-10%	S2-20%	S2-40%	S2-60%**
T_s (sec)	0.89	0.90	0.93	1.28	1.36	1.33	1.39	1.36	0.93	0.90	1.00	1.12
$\delta_{X,1}$ (mm)	12.6	29.5	164.5	226.7	74.2	110.2	196.2	429.4	9.9	22.7	59.5	253.1
$dRot_1$ (rad)	0.0015	0.0037	0.0224	0.0309	0.0083	0.0121	0.0210	0.0424	0.0003	0.0003	0.0002	0.0319
$\delta_{Y,1}$ (mm)	3.6	8.6	42.1	62.9	18.1	24.8	40.2	90.6	1.5	1.3	17.0	-
$\delta_{X,\mathrm{R}}$ (mm)	19.0	41.6	184.7	251.3	83.4	124.7	215.8	456.9	15.8	34.9	83.5	210.4
$dRot_\mathrm{R}$ (rad)	0.0017	0.0041	0.0234	0.0317	0.0086	0.0127	0.0220	0.0434	0.0003	0.0005	0.0001	0.0288
$\delta_{Y,\mathrm{R}}$ (mm)	4.8	9.8	45.6	72.3	20.0	31.6	46.7	107.3	3.4	2.2	16.2	-
$acc_{x,1}$ (g)	0.07	0.14	0.29	0.32	0.10	0.16	0.25	0.31	0.10	0.20	0.37	0.36
$acc_{x,\mathrm{R}}$ (g)	0.09	0.20	0.42	0.45	0.12	0.18	0.28	0.36	0.13	0.25	0.48	0.37

* results include residual displacement or diaphragm rotation
**δ and *dRot* are the values at axial failure of one of non-ductile columns, and peak acceleration excluded the spikes at failure.

5 EXPERIMENTAL VS. BLIND PREDICTION RESULTS

Table 6 summarises the test results for the parameters listed in Table 5. The measured fundamental period was identified from white noise tests conducted before each earthquake input using the 'Frequency Domain Decomposition' method (Brincker et al., 2000). Detailed description for the other parameters are found in the 'Results' document on the blind prediction competition website (http://www.quakecore.nz/blind-prediction-competition-2019-results/). Torsional response was observed in all the tests in Series-1A and Series-1B and as seen in the values of the diaphragm rotation. During the tests in Series-2, the specimen exhibited symmetric response until S2-40% (the third input). In fact, obvious torsional response was observed only during S2-60% and resulted in collapse of the specimen. Hence, the measured test results from S2-60% in Table 6 are the values at which axial failure of one of the non-ductile columns occurred (for discussion of these results see Suzuki et al. 2020). Figure 5 presents comparisons between the experimental and predicted results for the peak displacement in X-direction, peak diaphragm rotation, and peak acceleration in X-direction at geometric centre. Figure 6 shows box-and-whisker plots sorted by test.

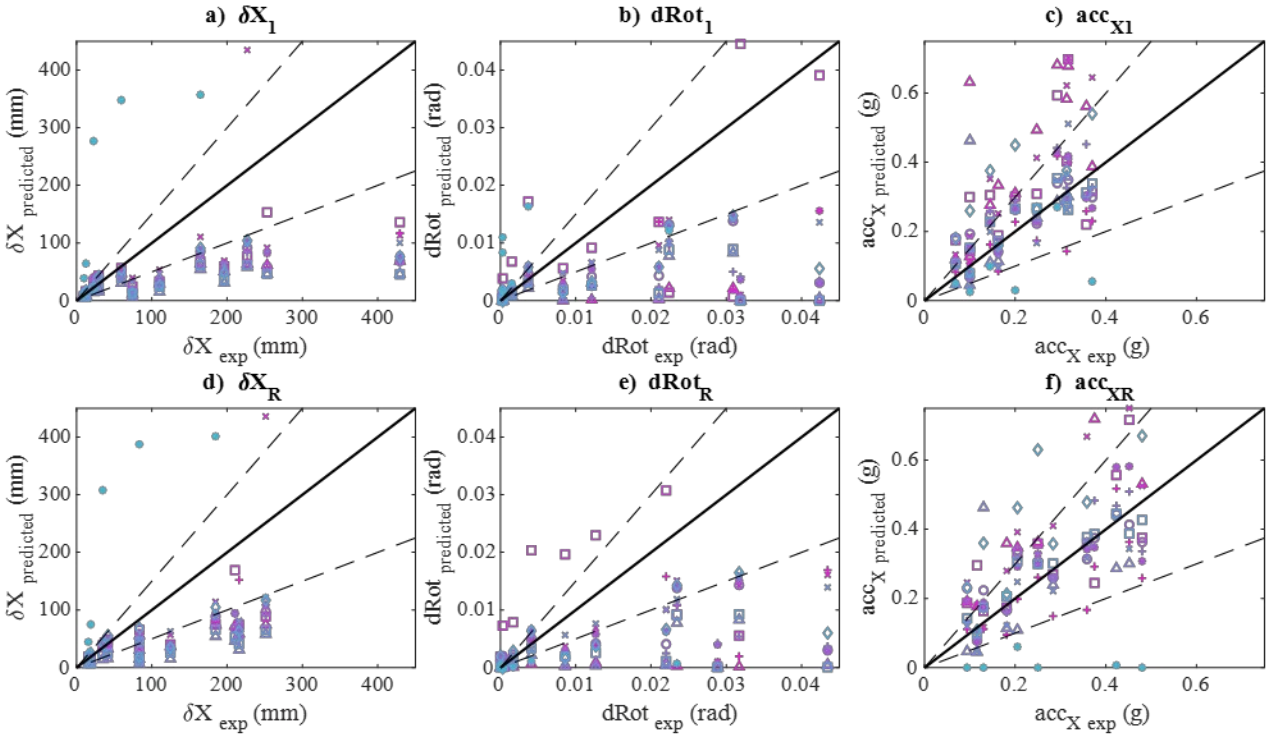

Figure 5 : Predicted VS experimental results (dashed lines indicate the boundary of ±50% offsets from the experimental values in Table 6)

The predicted displacement demand and diaphragm rotation for smaller inputs (10% and 20% inputs) in Series-1A and Series-2 are consistent with the experimental results: median values are close to the experimental values and there is a narrow distribution in the predicted results. On the other hand, the numerical analyses significantly underestimated the measured drifts and rotations for 60% inputs in Series-1A as well as all inputs in Series-1B; most of the predicted values were smaller than 50% of the experimental results. The underestimation in 1A-60% and 1A-60%-2 may have affected the predicted damage state compared to the experiment (flexural cracks and spalling of cover concrete at both ends of the first-story columns but no buckling or core crushing). This maybe the reason why torsional demands in Series-1B were not accurately captured during the analyses. This indicates that presence and extent of residual damage state of the structures may affect estimates of torsional response and resulting displacement demands for a damaged building. For Series-2, the predicted response of the frame was symmetric until S2-40%, which corresponds to the response observed in the tests. For these tests, the predicted values distributed within 50%-to-150% of the experimental results except that the displacements and diaphragm rotations were mostly within the 50-to-100% in S2-40%. In S2-60%, the predictions were unable to capture the collapse of the specimen resulting from brittle failure of the non-ductile columns and significant torsion; the predicted values were far less than those at axial failure in the test.

In contrast, the predicted acceleration values in Series-1B and Series-2 generally follow the trend of the experimental results (Fig. 5); most of the predicted values are within ±50% of the experimental results. This may be a result of a constant force demand after yielding in nonlinear response. Series-1A shows some overestimation and more variations in predicted values compared to the other test series. This may be because of variation in force demand on the masonry wall for different models; the modelling varied such as by multi struts, single strut with linear or nonlinear material properties and shell element.

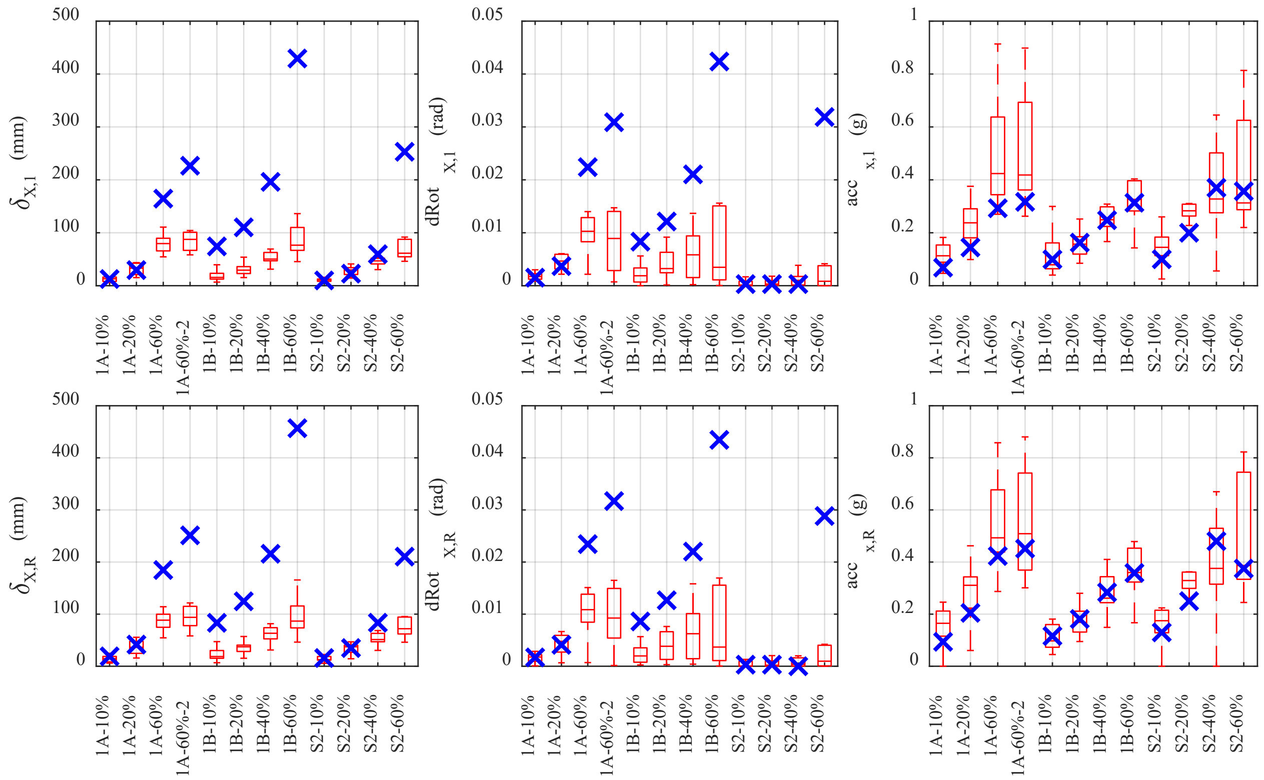

Figure 6 : Box-and-whisker plots of predicted results (×: indicates experimental results, the bottom and top edges of each box indicate the 25th and 75th percentiles and the centreline of the box indicates the median value, and outliers are not shown in the plots)

6 CONCLUSIONS

This paper presented an overview of a shake-table test program on two half-scale seven-story RC structures with torsional irregularities in relation to a blind prediction competition. The tests aimed to investigate inelastic torsional response of existing reinforced concrete buildings in Taiwan and New Zealand subjected to unidirectional ground excitation. The test results were compared with the numerical analyses submitted by 12 teams to better understand assessing inelastic torsional response using different methods and software packages. While analysis of the results is still ongoing, the preliminary findings are:

- Numerical analyses underestimated the drifts and diaphragm rotations in the experiment when the structures exhibited torsional response in the nonlinear range.
- Underestimates of damage in Series-1A may have resulted in less predicted drift demand in Series-1B. Further clarification is required to assess impact from prior damage on torsional demand.
- Prediction in the absolute acceleration in X-direction generally followed the trend from the experimental results. Some overestimation of accelerations in Series-1A may have resulted from uncertain force demand on the masonry wall.

7 ACKNOWLEDGEMENT

The blind prediction competition was supported under Flagship 3 funding from QuakeCoRE. The test program was made possible by research project funding (PI: Prof. Shyh-Jiann Hwang) from National Center for Research on Earthquake Engineering, Taiwan and Flagship 3 funding from QuakeCoRE, New Zealand Centre for Earthquake Resilience. Lastly, the first author would like to acknowledge the support for her PhD study through the University of Auckland Doctoral Scholarship.

REFERENCES

ASCE (2017). ASCE 41-17 “Seismic Evaluation and Retrofit of Existing Buildings”, ASCE, Reston.

ATC (2018). FEMA P-2012, “Assessing seismic performance of buildings with configuration irregularities.” FEMA, Washington D.C

Baker, J. W. (2011). “Conditional Mean Spectrum: Tool for Ground-Motion Selection.” Journal of Structural Engineering, 137(3), 322-331.

Brincker, R., Zhang, L., & Andersen, P. (2000). “Modal identification from ambient responses using frequency domain decomposition.” *Proceedings of the 18th International Modal Analysis Conference (IMAC), San Antonio, Texas*.

Castillo, R. (2004). "Seismic design of asymmetric ductile systems". PhD Dissertation, University of Canterbury. Department of Civil Engineering,

NZS 3101 (2006). Concrete structures standard, NZS 3101:2006., Standards New Zealand, Wellington, New Zealand

Paulay, T. (2001). “Some design principles relevant to torsional phenomena in ductile buildings.” Journal of Earthquake Engineering, 5(3), 273-308

Paulay, T. (1998). “Torsional mechanisms in ductile building systems.” Earthquake Engineering & Structural Dynamics, 27(10), 1101-1121.

PEER, "PEER Ground Motion Database.", University of Berkeley. https://ngawest2.berkeley.edu/

Sezen, H., & Moehle, J. P. (2004). “Shear strength model for lightly reinforced concrete columns.” Journal of Structural Engineering, 130(11), 1692-1703.

Suzuki, T., Elwood, K. J., Puranam, A. Y., Lee, H-J., Tsai, R-J., Hsiao, F-P. & Hwang S-J. (2020) “Seismic Response of Half-scale Seven-storey Reinforced Concrete Buildings with Torsional Irregularities”, to be submitted to *17th World Conference on Earthquake Engineering, Sendai, Japan*

Tarbali, K. & Bradley B. A. (2014). ”Representative Ground-motion Ensembles for Several Major Earthquake Scenarios in New Zealand.” Bullentin of NZSEE, 47(4), 231-252